Adsorption of water on O(2x2)/Ru(0001): thermal stability and inhibition of dissociation by H_2O-O bonding

Aitor Mugarza[1], Tomoko K. Shimizu[1,2,#], Pepa Cabrera-Sanfelix[3], Daniel Sánchez-Portal[4], Andres Arnau[4,5] and Miquel Salmeron[1,2,†]*

[1] Materials Sciences Division, Lawrence Berkeley National Laboratory, Berkeley, CA 94720

[2] Department of Materials Science and Engineering, University of California at Berkeley, CA 94720

[3]Donostia International Physics Center (DIPC), Manuel Lardizabal 4, San Sebastián 20018, Spain

[4] Unidad de Física de Materiales, Centro Mixto CSIC-UPV, Edificio Korta, Av. Tolosa 72, San Sebastián 20018, Spain

[5]Departamento de Física de Materiales UPV/EHU, Facultad de Química, Apartado 1072, San Sebastián 20080, Spain

MBSalmeron@lbl.gov

[*] Current address: Centre d'Investigació en Nanociència i Nanotecnologia CIN2 (ICN-CSIC), Campus UAB, 08193 Bellaterra Spain.

[#] Current address: Surface Chemistry Laboratory, RIKEN (The Institute of Physical and Chemical Research), 2-1-1 Wako, Hirosawa, Saitama 351-0198, Japan.

Adsorption of water on O(2x2)/Ru(0001)

†Corresponding author: Tel.: + 1-510-486-6230. Fax: +1-510-486-7268. E-mail:MBSalmeron@lbl.gov.

Abstract: The effect of preadsorbed oxygen on the subsequent adsorption and reactions of water on Ru(0001) has been studied using low temperature scanning tunneling microscopy and DFT calculations. Experiments were carried out for O coverages close to 0.25 ML. It was found that no dissociation of water takes place up to the desorption temperature of ~180-230 K. DFT calculations show that intact water on O(2x2)/Ru(0001) is ~ 0.49 eV more stable than the dissociation products, H and OH, at their preferred fcc and top adsorption sites.

1. Introduction

The practical relevance of wetting by water on different surfaces attracts a great deal of interest in the scientific community.[1,2] The delicate balance between water-surface and water-water interactions leads to a variety of water-solid interface structures.[3-7] This has lead to difficulties in the theoretical predictions of the structure and stability of water on many surfaces, as well as to controversial experimental results due to the formation of metastable and artificially induced structures. The literature on the adsorption of water on the Ru(0001) surface offers a clear example of these difficulties, and also how today a coherent vision of the theoretical and experimental results is finally being reached.[7-12] The emerging picture is that water adsorbs intact at low temperature, with the structure depending on the coverage. At low coverage flat, finite networks of hexamer rings are formed with maximized number of molecules with the plane parallel to the surface. Close to saturation of the monolayer water reorganizes in a buckled ice-like bilayer structure where molecules with the molecular plane parallel and perpendicular to the surface coexist in a 1:1 ratio, possibly arranged in a chain like structure.[7] Upon heating this layer undergoes partial dissociation and forms a more stable structure of mixed H_2O and

OH, forming elongated structures along preferred crystallographic directions of the hexagonal Ru surface.[7,13]

Although studies of water adsorption and reactions on the clean Ru surface are important, particularly in chemical and catalysis applications, it is equally important to study the adsorption on oxygen pre-covered surfaces, since water-oxygen interactions play an important role in chemistry and wetting. Several experimental groups have already shown that the addition of O dramatically affects the thermal stability of water, with very different results depending on the coverage.[1,12,14,15] X-ray photoemission spectroscopy (XPS) experiments indicate that the addition of small amounts of O, below ~0.20 ML, promotes the partially dissociated phase, while above this region the effect is the opposite and dissociation is inhibited.[15] However, a detailed understanding of the interaction between water and O is still missing and very few theoretical works deal with the interaction of co-adsorbed water and atomic oxygen.[16]

In this paper we report the results of a study, using a combination of scanning tunneling microscopy (STM) and density functional theory (DFT) calculations, of the thermal stability of water on O/Ru(0001) at oxygen coverages close to 0.25 ML where the transition between preferential dissociation and intact desorption occurs. We propose an explanation for the coverage dependent effect of O on the stability of water based on the energy balance between initial state and final products rather than on energy barriers.

2. Experimental Method

The experiments were performed using a home-built low temperature scanning tunneling microscope (STM).[17] The base pressure in the STM chamber was $< 2 \times 10^{-11}$ Torr, and all data were collected at 6 K using electrochemically etched W tips. In the STM body, the sample was heated when necessary with a resistor mounted near the sample plate, and the temperature was controlled with a Si diode mounted between the resistor and the sample. A single crystal Ru(0001) sample was cleaned in-situ following a previously established procedure.[17] The *p(2x2)*-O superstructure was obtained by exposing the sample to O_2 gas for 60 seconds at the pressure of 1×10^{-8} Torr at a sample temperature between 500-800 K. The

dosing parameters to create a 2x2 superstructure were calibrated by simultaneously tracking the intensity of the 2x2 spots in the LEED pattern while dosing. The structure was subsequently checked by STM before dosing water.

Water was dosed through a leak valve and a dosing tube pointing towards the sample inside the STM body. The source was Milli-Q water in a glass tube that was further purified by repeated cycles of freezing, pumping and thawing prior to introduction in the microscope chamber.

3. Theoretical Method

Density functional theory (DFT) calculations were performed using the Vienna Ab initio Simulation Package (VASP),[18-20] within the Perdew-Wang 1991 (PW91) version of the general gradient approximation (GGA).[21] The projector augmented wave (PAW)[22,23] method was used to describe the interaction of electrons with Ru, O and H atoms.

A symmetric slab of seven Ru layers and the same amount of vacuum was used to represent the Ru (0001) surface. The oxygen and water species are placed on each surface of the symmetric slab. A plane-wave cutoff of 400 eV, a 3x3x1 k-point sampling and a lateral 4x4 supercell have been used for calculations on both clean Ru(0001) and O(2x2)/Ru(0001) surfaces. The size of the lateral supercell allows for the study of low water coverages down to 0.0625 ML. In the (2x2) structure previous to water deposition, the oxygen atoms are located at hcp sites, 1.17 Å above the Ru topmost layer. All geometries have been optimized by allowing relaxation of all degrees of freedom of the top and bottom Ru layers and adsorbates until residual forces were smaller than 0.03 eV/Å. This procedure was checked in previous work to be accurate enough.[24,25]

The adsorption energies of the water molecule and the dissociated fractions, E_{ads}, are calculated from:

$$E_{ads} = -(E_{adsorbate+surface} - E_{surface} - E^{isol}_{adsorbate}) \qquad (1)$$

where $E_{adsorbate+surface}$ is the energy of the optimized combined system, $E_{surface}$ the energy of the relaxed Ru(0001) or O(2x2)/Ru(0001) surface, and $E^{isol}_{adsorbate}$ the energy of the relaxed species isolated in vacuum

calculated using the same 4x4 supercell. In the calculations of H and OH in vacuum, spin polarization has been taken into account.

The STM simulations were performed using the Tersoff-Hamann approximation.[26,27]

4. Results

The O(2x2)/Ru(0001)

An example of the *p(2x2)*-O structure prepared as described in the experimental section is shown in Figure 1 a. The tunneling conductance is lower over the O atoms, which brings the tip closer to the surface, giving rise to dark spots in the gray scale representation. Several defects are present in this image. O-vacancies appear as bright triangular protrusions with a density of 0.007 ML relative to the density of Ru atoms. Another defect appears as a dark spot surrounded by 3 O atoms (marked by a circle in the figure). Its concentration can vary between 0.002 ML, as in this image, and 0.01 ML, depending on the experimental conditions. Pairs of impurities separated by two lattice constants can be frequently observed. By comparison of experimental and simulated images (see below) and from its easy displacement by application of voltage pulses above 100 mV we identify these defects as atomic H sitting in the open fcc sites of the 2x2 unit cell.

There is the possibility of atomic C being present as an impurity substituting O in the 2x2 lattice. Our Ru surface contained around 0.03 ML of C prior to dosing O.[17] Since both C and O occupy hcp hollow sites and have similar contrast in the STM images, substitutional C in the *p(2x2)*-O superstructure is not easy to detect by simple inspection of the images. If all C atoms would stay on the surface after dosing O they would represent about 12 % of the adatoms in the 2x2 superstructure and, therefore, we believe that they do not affect our conclusions.

In Figure 1 a the bright and sharp spot marked with an arrow is a water molecule used for the identification of the adsorption site of H. Knowing that water adsorbs on top sites[25] and O on hcp sites,[24] the images indicate then that H adsorbs on fcc hollow sites, in agreement with the minimum-energy adsorption site calculated for H, both on the clean and O-covered Ru(0001) surface, although the

binding energy decreases from 2.90 eV to 2.60 eV in the presence of preadsorbed hcp O atoms (see Table 1).

Adsorption of water at 20 K

The coverage dependent adsorption geometry and energy of water has been presented elsewhere;[25] therefore it will only be briefly reviewed here. When the water coverage is below 0.25 ML, the molecules adsorb on top Ru sites inside the O(2x2)/Ru(0001) unit cell with the molecular plane nearly parallel to the surface and forming H-bonds with two of the neighboring O atoms of the 2x2 unit cell. This H-bonding contributes an additional binding energy of 0.14 eV, as compared to the energy on the clean Ru(0001).[28] As the water coverage increases and the exposed Ru top sites are filled, water forms a 2x2 structure over that of the O-layer. There is no direct water-water bonding in this structure. Some fuzzy lines observed in images acquired after dosing water at 20 K suggest the presence of unstable monomers or clusters that are dragged by the tip during scanning. The sample was then annealed to 75-140 K in order to bring the system into a stable configuration. This eliminated the unstable monomers, probably by facilitating their diffusion to stable 2x2 top sites without affecting the overall structure. A similar stabilization of the adsorption configuration in this temperature range has also been reported for water on O(2x2)/Ni(111).[29,30] Figures 1 b and c show the surface after depositing 0.07 ML and 0.23 ML of water and annealing to 140 K and 75 K, respectively. The coverage refers to immobile molecules in the 2x2 structure. It does not include the weakly bound molecules that are dragged by the tip and produce the fuzzy lines in the STM image.

In contrast to this observation, theoretical calculations indicate the existence of a stable configuration for 0.5 ML of water with the extra 0.25 ML consisting of water molecules forming two H-bonds: one to the molecules bound to the Ru on top sites (i.e., forming dimers) and the other to the pre-adsorbed O, instead of direct bonding to Ru in the available fcc or hcp hollow sites.[25] The absence of such a structure in our STM images might indicate that its formation is kinetically hindered by an energy barrier. To stabilize this second phase a higher water coverage and higher temperature treatment than the one used

in these experiments would be necessary. The existence of two different adsorption states is in line with the peak shifts in temperature programmed XPS experiments at high water coverage reported by Gladys et al.[15] The shift in the water-related O peak at 175 K could be due to the desorption of the H-bonded water in the dimer, whereas the peak of the most stable, Ru-bonded water forming the 2x2 superstructure would remain up to higher temperatures. Further work is required to clarify the possible relation between these observations and the calculated 0.5 ML structure.

Thermal annealing

In these experiments the surface was annealed to different temperatures and imaged after cooling back to 6 K. The initial coverage of water in each of these experiments was 0.06 ML. In Figure 2 we show images obtained after annealing to 100 K, 180 K, 200 K and 230 K, as indicated. Figure 3 displays the H_2O and H coverage deduced from the images as a function of temperature. The H coverage was obtained by counting the isolated H atoms and, in case of clustering, assuming a 1x1 phase, which sets an upper limit.[31]

Figure 2 a shows the surface after annealing to 100 K. The appearance is identical to the pre-annealed surface, i.e., monomers adsorbed on Ru top sites of the 2x2 unit cells. The H concentration increased from 0.004 to 0.014 ML. Since the water coverage remained unchanged, we attribute the increase in H to adsorption of H_2 displaced from the microscope body during annealing.

After annealing to 180 K (Figure 2 b), the water coverage decreased from 0.063 ML to 0.035 ML. This decrease was not accompanied by a change in H concentration. We also did not see any decrease in the pre-adsorbed O concentration. The possibility of having OH substitutional or interstitial in the *p(2x2)*-O lattice seems energetically excluded by our first principles calculations, where adsorption of H on top of the O atoms is 1.2 eV less favorable than the adsorption at fcc site. To better understand the outcome of these experiments, simulated STM images for both H_2O and OH + H were compared. The latter was calculated for different OH-H distance, which did not produce any important change in the appearance of the species (with OH and H in the same and in separate O(2x2) unit cells). Images for

H_2O and OH + H are displayed in Figure 4 and 4 . Although both H_2O and OH appear as bright dots, the apparent height for OH is lower than for H_2O. This decrease in apparent height is consistent with the decrease observed from H_2O to OH on the clean Ru(0001) surface,[32] although in this latter case the differences are larger. Since no change in apparent height of the bright features is observed during the annealing series, we exclude the possibility of having OH on this surface.

Annealing to 200 K results in the nearly complete desorption of water, with a residual coverage of 0.01 ML, which is again not accompanied by any increase of H concentration (Figure 2). Finally, after annealing to 230 K, all water molecules are desorbed. It produced also a few changes in the structure of the surface; for example, the O vacancies appear to coalesce into small clusters (Figure 2). Although their concentration of approximately 0.015 ML is within the range found in other O precovered surfaces before dosing water, a slight increase of O vacancies during annealing is possible and could explain the decrease of H of 0.005 ML after annealing to 230 K via water formation by recombination. H impurities also coalesce in small clusters during the annealing (dark clusters in Figure 2 b-d). The remaining bright dots are unidentified impurities also found on the surface before water dosing (indicated by an arrow in Figure 5 a). Unlike water molecules, they cannot be manipulated by V pulses. In any case, the important conclusion that can be extracted from our thermal treatment experiment is that water gradually desorbs intact in the temperature range of 180-230 K. The results are again in agreement with the gradual decrease of XPS peak corresponding to the most stable water phase observed in the same temperature range in Ref. 15.

DFT calculations confirm the preferential intact water adsorption versus dissociation on a O(2x2)/Ru(0001) surface, contrary to what occurs on clean Ru(0001) surfaces. The results are summarized in Table 1. Notice that the water coverage of 0.0625ML, considered in the calculations, is low enough to represent the adsorption of an isolated monomer. We estimated that the interaction with periodic images varies the adsorption energy of the molecule by less than 8 meV, which is inside the error bar for our calculated adsorption energies. On the clean Ru(0001) surface fcc sites are energetically preferred by both the H and OH fractions although hcp sites are also possible for OH, since they are just

26 meV less stable than fcc. Actually, when OH and H are co-adsorbed as first neighbors it becomes energetically favorable (by ~70 meV) for OH and H to occupy neighboring hcp and fcc sites, respectively, (configuration c in Table. 1) instead of sitting on neighboring fcc sites. Dissociation is ~0.35-0.39 eV more favorable than non-dissociative water adsorption, depending on the distance between the two products, in agreement with previous calculations.[9] However, the situation is reversed on the O-covered surface, where non-dissociative adsorption is more favorable by ~ 0.47-0.49 eV. The distance dependent energy observed in both cases reflects a slightly attractive interaction between OH and H. Notice that the OH adsorption site changes to top for the O(2x2)/Ru(0001) surface. A possible mechanism to explain the preference for the top site is the formation of an extended hydrogen bond, ~ 2.58 Å, between the OH fraction and the O atoms in the surface, as it is observed in the calculations and schematically shown in Figure 4 c. Zero point energy contributions would reduce these energy differences by less than 0.1 eV,[33] thus leaving the main result unaltered.

The thermal stability of molecular water on the O-precovered surface could driven by two different factors. One is related to the modification of the dissociation energy barrier by the presence of O. The importance of clustering for the dissociation of water has already been demonstrated both experimentally and theoretically.[3,9,34-40] For clean Ru(0001), water clustering is essential to reduce the dissociation barrier from 0.85 eV to 0.50 eV, which is below the desorption barrier.[9] When O covers the surface with a 2x2 lattice, the situation is totally different. Clustering of molecules is not observed due to the larger adsorption energy that immobilizes the molecule in the 2x2 unit cell. The inhibition of clustering on this patterned surface therefore would favor the quenching of dissociation.

The second factor is the modification of the relative adsorption energies between the intact and dissociated water. In the case of O(2x2)/Ru(0001) we have shown that, not only intact water is stabilized by ~ 0.14 eV respect to the clean Ru(0001) by forming two extended H-bonds to adjacent chemisorbed O atoms, but the adsorption energy of the dissociated products OH + H is modified such that dissociation becomes energetically unfavored in the O(2x2) covered surface. Thus, regardless of energy barriers, inhibition of dissociation can be explained in terms of relative adsorption energies alone.

Adsorption and dissociation of water on a defective O(2x2) surface

In order to study the nature of the sites leading to dissociation of water, we prepared a surface with an O coverage below the saturation of the O(2x2) structure exhibiting small patches of clean Ru. An image of such a surface is shown in Figure 5 a, with O-vacancies, comprising 2% of O in the 2x2 structure, visible in the form of triangular features (medium-bright contrast in the image) isolated or in clusters. To this surface, 0.003 ML of water were added, which produced the brighter spots. When the water coverage was increased to 0.065 ML and annealed to 100 K, as in Figure 5 b, the water in the O(2x2) areas remained intact. However, the molecules adsorbed on the clean Ru patches reacted to create new structures with brighter perimeter, which is characteristic of mixed H_2O-OH clusters. These are very similar to those formed on the clean Ru surface consisting a mixture of H_2O and OH.[13,32] This process is amplified by heating to 140 K, as shown in Figure 5 c. The formation of the mixed H_2O-OH clusters is in stark contrast to the case of the complete O(2x2), where no dissociation was observed. Indeed calculations indicate that on a Ru(0001) surface with 0.0625 ML oxygen coverage, corresponding to a O(4x4) supercell, dissociative adsorption is energetically favored by about 0.2 eV.[41]

5. Conclusions

Our combined STM studies and DFT calculations of water adsorption on O(2x2)/Ru(0001) show that water remains intact up to 230 K, in contrast to the partial dissociation observed on the clean Ru(0001). Water molecules, bound to the available Ru top site and stabilized by H-bonding to the two neighboring O, gradually desorb in the temperature range of 180-230 K. We have shown that the presence of O vacancies is necessary for dissociation to occur. DFT calculations indicate that the change in the relative adsorption energies of intact and dissociated water induced by the presence of O is large enough to prevent dissociation, excluding any energy barrier modification effect. The calculations show also that on more open structures, such as the O(4x4) exposing several Ru atoms, dissociation of water is again favorable.

Acknowledgements

This work was supported by the Director, Office of Energy Research, Office of Basic Energy Sciences, Materials Sciences Division, of the U.S. Department of Energy under Contract No. DE-AC02-05CH11231. A.M. was financed by the Marie Curie Outgoing International Foundation, Project No. 514412, through the Institut de Ciencia de Materials de Barcelona- CSIC.

Figures and tables

Table 1. Calculated adsorption energies for a water molecule and its dissociation products (H and OH) on Ru(0001) and O(2x2)/Ru(0001) surfaces. The single phases are calculated in a 4x4 unit cell. The energy balance for the coadsorption of OH + H (ΔE) is defined by $\Delta E = E_{ads.H} + E_{ads.OH} - E_{H2O\_.break}$; where $E_{H2O\_.break}$ is the energy cost to break a O-H bond in the water molecule in the gas phase (~5.58 eV). The positive values of ΔE indicate energy release (exothermicity). The last row corresponds to the comparison between intact adsorption and dissociated water fractions adsorbed infinitely distant and in nearest neighbor hcp-fcc sites (in parenthesis). Negative values indicate preferred dissociation over intact water adsorption, whereas the positive difference favors molecular adsorption.

	Ru(0001)	**O(2x2)/Ru(0001)**
E_{ads_H2O} (eV)	0.47 (top)	0.62 (top)
E_{ads_H} (eV)	2.90 (fcc)	2.60 (fcc)
E_{ads_OH} (eV)	3.50 (fcc)	3.10 (top)
ΔE [a] (eV)	0.82 (fcc/fcc)	0.13 (top/fcc)
ΔE [b] (eV)	0.86 (fcc/fcc)	0.13 (top/fcc)
ΔE [c] (eV)	0.87 (hcp/fcc)	0.15 (top/fcc)
$E_{ads\_H2O} - \Delta E$ [a] (eV)	-0.35	0.49

$E_{ads\_H_2O} - \Delta E$ [c] (eV)	-0.39	0.47

[a] OH and H in a separate phase (infinite OH-H distance)

[b]OH and H coadsorbed in a 4x4 unit cell (close distance).

[c]OH and H coadsorbed in a 2x2 unit cell (as close as possible).

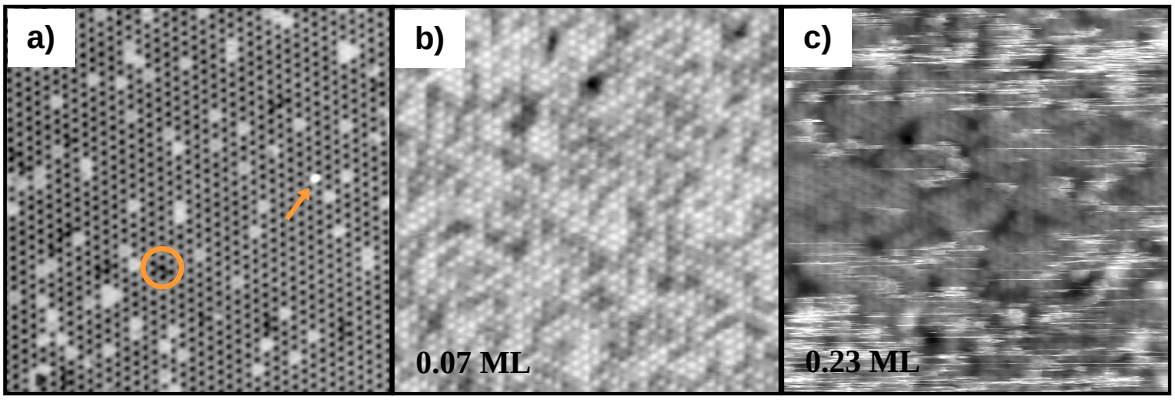

Figure 1. STM images (20 nm x 20 nm) of: a) O(2x2) superstructure on Ru(0001). O vacancies (bright triangular features) can be observed isolated or forming small aggregates. H atoms are also present (faint black spots marked by a circle). A water molecule, introduced for identification purposes is visible as the bright spot marked with an arrow. Tunneling conditions: 184 mV, 102 pA. b) After dosing 0.07 ML of water followed by annealing to 140 K. Water monomers order in a 2x2 structure intercalated with the O 2x2. Tunneling condition: –218 mV, 95 pA. c) After dosing 0.23 ML of water on the surface shown in b) followed by annealing to 75 K. The coverage is referred to the immobile molecules in the 2x2 structure (ordered background). In addition to these, streaky lines are visible due to weakly bound molecules being dragged by the tip during scanning. Tunneling condition: 69 mV, 46 pA.

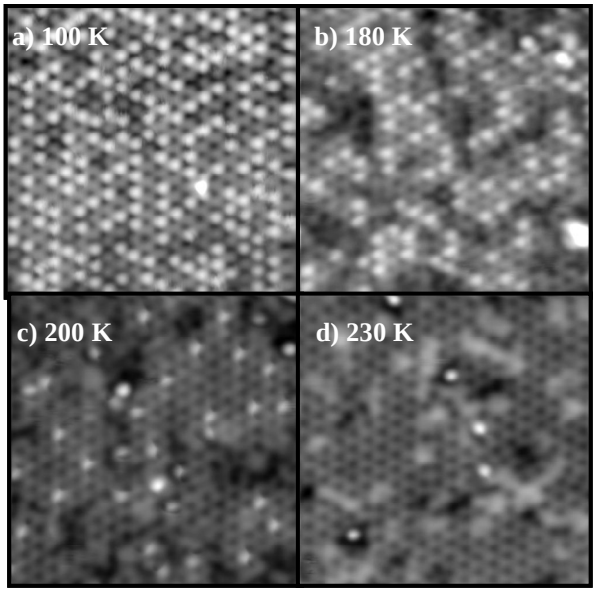

Figure 2. Thermal evolution of a 0.063 ML of water on the O(2x2) Ru surface dosed at 20 K followed by annealing to: a) 100 K, b) 180 K, c) 200 K, and d) 230 K. Neither clustering nor dissociation of water is observed. Complete desorption takes place at 200-230 K. During annealing the H impurities (dark spots in b) and oxygen vacancies (grey clusters in d) coalesce into small clusters. The bright dots in d) are unidentified impurities also found before dosing water (indicated by an arrow in Figure 5 a). Image size is 10x10 nm. Tunneling conditions from a) to d): 40 mV, 100 pA; 100mV, 100 pA; 50 mV, 400 pA; 50 mV, 345 pA.

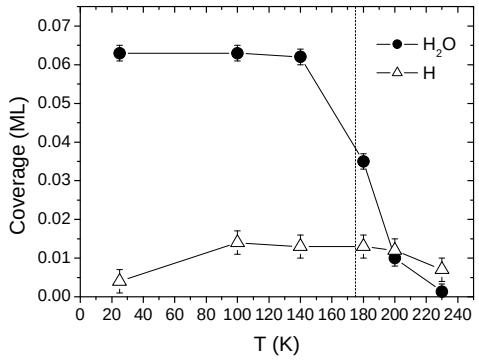

Figure 3. Water and hydrogen coverage as a function of annealing temperature of 0.063 ML of water dosed at 25 K.

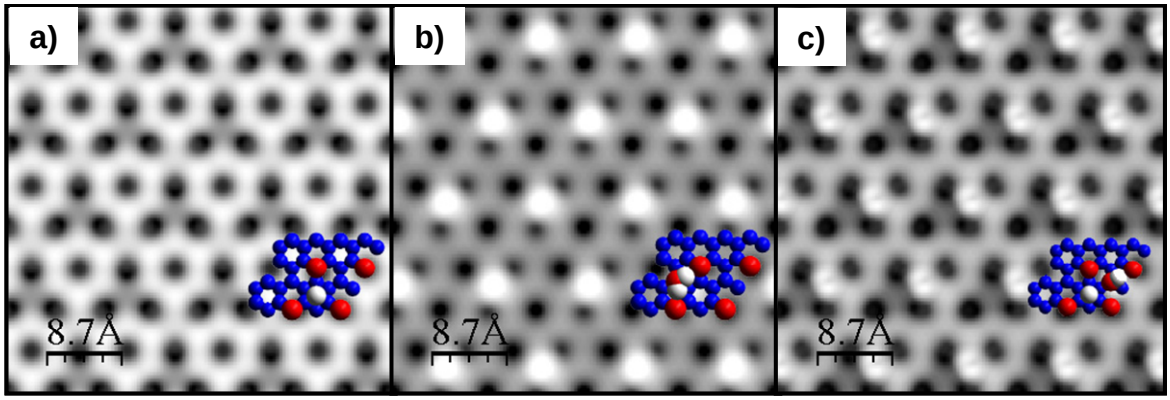

Figure 4. Simulated STM images at constant current for a voltage of 150 meV on a 4x4 unit cell of the (2x2)O/Ru(0001) surface. (a) One H atom adsorbed on each fcc site of the 2x2 unit cell. (b) H_2O on each top site. (c) OH on a top site and H on a fcc site.

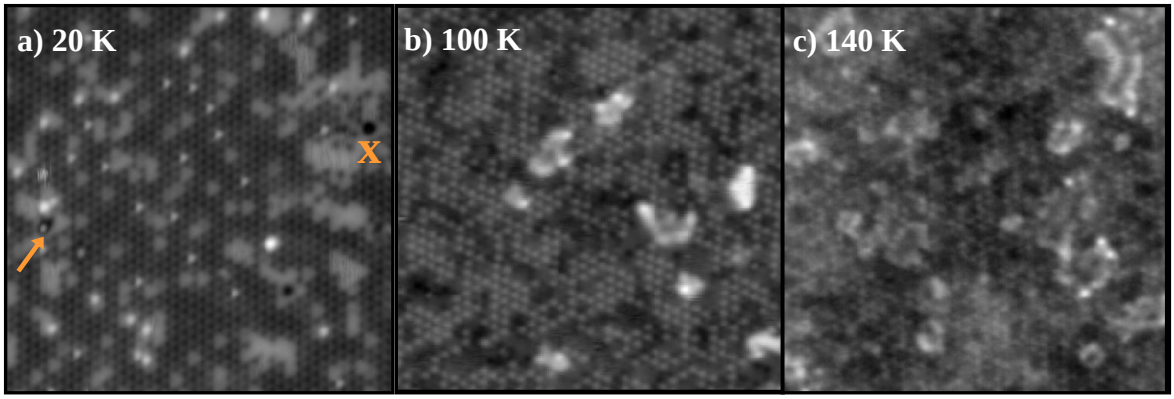

Figure 5. Thermal evolution of water on an incomplete O(2x2) adlayer containing 2% of O vacancies. The O-vacancies are visible as triangular medium bright features either isolated or forming aggregates that expose the clean Ru(0001) patches. A few unidentified impurities are also found on the surface before dosing water (marked by arrows in a)). Image size is 20 nm x 20 nm. (a) 0.003 ML of water dosed at 20 K. Water monomers adsorb both on the areas covered by the O(2x2) structure and on vacancy islands. In the latter case, they tend to attach to the O atoms at the border. Tunneling condition: 106 mV, 152 pA. (b) Increasing the water coverage to 0.069 ML and annealing to 100 K. A 2x2 structure of water is formed in the O(2x2) covered areas, and some water clusters are observed on the clean Ru patches. Tunneling condition: 150 mV, 104 pA. (c) After annealing the previous surface, in b), to 140 K. The elongated clusters with bright perimeters on the clean Ru patches are characteristic of the

partially dissociated clusters observed on the clean Ru(0001) surface.[13,32] On the O(2x2) areas intact water monomers are still visible. Tunneling condition: 103 mV, 204 pA.

References

(1) Thiel, P. A.; Madey, T. E. *Surf. Sci. Rep.* **1987**, *7*, 211-385.
(2) Henderson, M. A. *Surf. Sci. Rep.* **2002**, *46*, 5-308.
(3) Meyer, B.; Marx, D.; Dulub, O.; Diebold, U.; Kunat, M.; Langenberg, D.; Wöll, C. *Angew. Chem. Int. Ed.* **2004**, *43*, 6642-6645.
(4) Mehlhorn, M.; Morgenstern, K. *Phys. Rev. Lett.* **2007**, *99*, 246101.
(5) Cerdá, J.; Michaelides, A.; Bocquet, M. L.; Feibelman, P. J.; Mitsui, T.; Rose, M.; Fomin, E.; Salmeron, M. *Phys. Rev. Lett.* **2004**, *93*, 116101.
(6) Yamada, T.; Tamamori, S.; Okuyama, H.; Aruga, T. *Phys. Rev. Lett.* **2006**, *96*, 036105.
(7) Haq, S.; Clay, C.; Darling, G.; Zimbitas, G.; Hodgson, A. *Phys. Rev. B* **2006**, *73*, 115414.
(8) Feibelman, P. J. *Science* **2002**, *295*, 99.
(9) Michaelides, A.; Alavi, A.; King, D. A. *J. Am. Chem. Soc.* **2003**, *125*, 2746-2755.
(10) Faradzhev, N. S.; Kostov, K. L.; Feulner, P.; Madey, T. E.; Menzel, D. *Chem. Phys. Lett.* **2005**, *415*, 165-171.
(11) Weissenrieder, J.; Mikkelsen, A.; Andersen, J. N.; Feibelman, P. J.; Held, G. *Phys. Rev. Lett.* **2004**, *93*, 196102.
(12) Clay, C.; Haq, S.; Hodgson, A. *Chem. Phys. Lett.* **2004**, *388*, 89-93.
(13) Andersson, K.; Fomin, E.; Tatarkhanov, M.; Shimizu, T. K.; Mugarza, A.; Odelius, M.; Cerdá, J.; Ogasawara, H.; Petterson, L. G. M.; Ogletree, D. F.; Salmerón, M.; Nilsson, A. *In preparation* **2007**.
(14) Kretzchmar, K.; Sass, J. K.; Gradshaw, A. M.; Holloway, S. *Surf. Science.* **1982**, *115*, 183.
(15) Gladys, M.; Mikkelsen, A.; Andersen, J.; Held, G. *Chem. Phys. Lett.* **2005**, *414*, 311-315.
(16) Wang, G.-C.; Tao, S.-H.; Bu, X.-H. *Journal of Catalysis* **2006**, *244*, 10-16.
(17) Shimizu, T. K.; Mugarza, A.; Cerdá, J. I.; Heyde, M.; Qui, Y.; Schwarz, U. D.; Ogletree, D. F.; Salmeron, M. *J. Phys. Chem. C, submitted* **2007**.
(18) Kresse, G.; Hafner, J. *Phys. Rev. B* **1993**, *47*, 558-561.
(19) Kresse, G.; Hafner, J. *Phys. Rev. B* **1994**, *49*, 14251-14269.
(20) Kresse, G.; Furthmuller, J. *Phys. Rev. B* **1996**, *54*, 11169-11186.
(21) Perdew, J. P.; Chevary, J. A.; Vosko, S. H.; Jackson, K. A.; Pederson, M. R.; Singh, D. J.; Fiolhais, C. *Phys. Rev. B* **1992**, *46*, 6671-6687.
(22) Blochl, P. E. *Phys. Rev. B* **1994**, *50*, 17953-17979.
(23) Kresse, G.; Joubert, D. *Phys. Rev. B* **1999**, *59*, 1758-1775.
(24) Calleja, F.; Arnau, A.; Hinarejos, J. J.; de Parga, A. L. V.; Hofer, W. A.; Echenique, P. M.; Miranda, R. *Phys. Rev. Lett.* **2004**, *92*, 206101.
(25) Cabrera-Sanfelix, P.; Sánchez-Portal, D.; Mugarza, A.; Shimizu, T. K.; Salmeron, M.; Arnau, A. *Phys. Rev. B* **2007**, *76*, 205438.
(26) Tersoff, J.; Hamann, D. R. *Phys. Rev. Lett.* **1983**, *50*, 1998-2001.
(27) Tersoff, J.; Hamann, D. R. *Phys. Rev. B* **1985**, *31*, 805-813.
(28) footnote1.
(29) Nakamura, M.; Ito, M. *Phys. Rev. Lett.* **2005**, *94*, 033501.
(30) Nakamura, M.; Tanaka, M.; Ito, M.; Sakata, O. *J. Chem. Phys.* **2005**, *122*, 224703.

(31) footnote2.
(32) Shimizu, T. K.; Mugarza, A.; Ogletree, D. F.; Salmeron, M. *Submitted* **2007**.
(33) Feibelman, P. J. *Phys. Rev. B* **2003**, *67*, 35420.
(34) Andersson, K.; Gómez, A.; Glover, C.; Nordlund, D.; Öström, H.; Schiros, T.; Takahashi, O.; Ogasawara, H.; Petterson, L. G. M.; Nilsson, A. *Surf. Sci.* **2005**, *585*, L183-L189.
(35) Kato, H. S.; Shiraki, S.; Nantoh, M.; Kawai, M. *Surf. Sci.* **2003**, *544*, L722-L728.
(36) Ren, J.; Meng, S. *J. Am. Chem. Soc.* **2006**, *128*, 9282-9283.
(37) Odelius, M. *Phys. Rev. Lett.* **1999**, *82*, 3919.
(38) Michaelides, A.; Hu, P. *J. Am. Chem. Soc.* **2001**, *123*, 4235-4242.
(39) Lindan, P. J. D.; Zhang, C. *Phys. Rev. B* **2005**, *72*, 75439.
(40) Akagaki, K.; Tsukada, M. *Surf. Sci.* **1999**, *438*, 9-17.
(41) Cabrera-Sanfelix, P.; Sanchez-Portal, D.; Arnau, A. **2008**.